

Traffic Abstractions of Nonlinear Event-Triggered Control Systems with Disturbances and Uncertainties

Giannis Delimpaltadakis, and Manuel Mazo Jr.*

April 12, 2021

Abstract

Scheduling communication traffic in networks of event-triggered control (ETC) systems is a very challenging task, as the exact sampling time instants are generally unknown (as opposed to periodic sampling). In previous work, finite-state systems (abstractions) were created, capturing the traffic generated by linear time-invariant ETC systems with a specific type of triggering function. It has been shown that such abstractions can be used for scheduling traffic in networks of ETC loops. In this work, we significantly extend this framework, by proposing a methodology for abstracting general nonlinear ETC systems with disturbances, uncertainties and general triggering functions.

1 Introduction

The widespread use of networked control systems (NCS) and shared digital platforms, that act as controllers for multiple control loops simultaneously, asks for effective solutions regarding consumption of bandwidth and computational resources. Specifically, periodic sampling seems inefficient, as it often leads to unnecessary sampling, communication and control computation. To tackle this inefficiency, the community has shifted its focus to aperiodic sampling strategies; the most prominent ones being Event-Triggered Control (ETC) [1–7] and Self-Triggered Control (STC) [8–13]. For an introduction to ETC and STC, the reader is referred to [14].

Both ETC and STC determine sampling instants in a way such that communication between the sensors and the controller is minimized, while certain performance specifications are met (e.g. stability, convergence rate, etc.). Particularly in ETC, the sensors measure continuously the system's state, and the sampling instants are determined by the satisfaction of a certain state-dependent *triggering condition*, which is evaluated at the sensors' end. On the other hand, in STC the controller uses the previous measurement to decide the next sampling instant. However, due to this open-loop nature of sampling, STC is generally considered less robust than ETC, as the controller does not employ any (possibly critical) information on the state between sampling instants.

Even though the vast research on ETC has shown promising results, there are still open problems that stand in the way of it becoming the main sampling paradigm in NCS. One such problem is the scheduling of communication traffic in networks of ETC loops. In contrast to periodic sampling, where the sampling instants are known by construction, ETC sampling instants are generally

*The authors are with the Delft Center for Systems and Control, Delft University of Technology, Delft 2628CD, The Netherlands. Emails: {i.delimpaltadakis, m.mazo}@tudelft.nl. This work is supported by the ERC Starting Grant SENTIENT (755953).

unknown, due to the event-based nature of sampling. This renders scheduling of ETC traffic a challenging problem. One way of approaching it is the controller/sampler/scheduler co-design techniques [15–21]. According to such strategies, given a network of control loops, the controllers, the sampling instants and the scheduler are all designed in a coupled manner, such that resource utilization is efficient, while certain performance specifications are satisfied. However, such approaches show a lack of versatility, as for example the whole design process has to be applied from scratch, when a new control loop joins the network.

An essentially different line of work is the one proposed in [22] and [23]. According to this approach, ETC systems are abstracted by finite-state *quotient systems* (or *abstractions*), capturing the ETC systems’ sampling behaviour. In [23], it was shown that such abstractions are equivalent to timed automata and can be readily employed for traffic scheduling. This approach is more versatile, as the abstraction of each system in the network is computed only once, and does not change with the presence of a new system. For the construction of the abstraction, the system’s state-space is partitioned into a finite number of regions \mathcal{R}_i , which are associated to the abstraction’s states. For each region \mathcal{R}_i , a time interval $[\underline{\tau}_i, \bar{\tau}_i]$ is determined such that it contains all possible inter-sampling times that correspond to each state contained in \mathcal{R}_i . These intervals serve as the abstraction’s output. Finally, the abstraction’s transitions are determined via reachability analysis (e.g. see [24, 25]), conducted with the regions \mathcal{R}_i as initial sets. The work in [22] carried out the task of abstracting linear time-invariant (LTI) ETC systems with quadratic triggering functions, by partitioning the state space into conic regions \mathcal{R}_i and deriving the intervals $[\underline{\tau}_i, \bar{\tau}_i]$ by solving LMIs.

In this work, building on tools developed in [12, 13, 26] and [27], we significantly extend the aforementioned framework by creating traffic abstractions of general nonlinear ETC systems with disturbances, uncertainties and general triggering functions. A preliminary version of the present article has been presented in [26], which focused only on unperturbed homogeneous systems with quadratic triggering functions. Note that compared to [22] and [23] we use a different approach for determining the intervals $[\underline{\tau}_i, \bar{\tau}_i]$ and partitioning the state space. Here, the system’s state space is partitioned into a finite number of polytopes \mathcal{R}_i . To determine the lower bounds $\underline{\tau}_i$ of inter-sampling times of regions \mathcal{R}_i , first the system is embedded in a higher-dimensional space where it is rendered homogeneous (homogenization procedure [27]), by adding an extra dummy variable w . The original system’s state space is then mapped to the $w = 1$ -hyperplane of the extended system’s state space. By employing inner approximations of *isochronous manifolds* (hypersurfaces which correspond to a uniform inter-sampling time), previously derived in [12], and the scaling law of inter-sampling times of homogeneous ETC systems (see [11]), the lower bounds $\underline{\tau}_i$ for regions \mathcal{R}_i (which are represented by polytopes on the $w = 1$ -hyperplane) are determined. The upper bounds $\bar{\tau}_i$ and the transitions between the abstraction’s states are obtained concurrently via reachability analysis, as proposed in [26]. Finally, to deal with disturbances and uncertainties, we employ differential inclusions (DIs), as proposed in [13], where theoretical results of [27] and [12] (e.g. homogenization procedure, scaling law, approximations of isochronous manifolds, etc.) were extended to perturbed uncertain systems.

Even though the abstraction is constructed offline, it has to be noted that our construction suffers from the curse of dimensionality (as does [22]), due to the way that the state space is partitioned. However, it serves as a significant contribution to versatile scheduling of ETC traffic, as it extends its applicability, from LTI systems with quadratic triggering functions, to general nonlinear systems with disturbances, uncertainties and general triggering functions. Moreover, performed numerical simulations indicate that for systems of small to moderate dimensionality, the algorithm that computes the abstraction terminates relatively fast. Finally, in Section 8, we discuss possible ways of taming the curse of dimensionality, building on this paper’s proposed methodology.

2 Notation and Preliminaries

2.1 Notation

The set \mathbb{R}_0^+ denotes the non-negative reals, while the set \mathbb{R}^+ denotes the strictly positive reals. We use small Latin characters to denote points in \mathbb{R}^n (e.g. $x \in \mathbb{R}^n$) and Greek characters to denote trajectories (e.g. $\xi(t)$, with $\xi : \mathbb{R}_0^+ \rightarrow \mathbb{R}^n$). The Euclidean norm of $x \in \mathbb{R}^n$ is denoted by $|x|$. For vectors, we also use the notation $(x_1, x_2) = [x_1^\top \ x_2^\top]^\top$. With the symbol $\exists!$, we denote existence and uniqueness. For a set $X \subseteq \mathbb{R}^n$, $\text{int}(X)$ denotes its interior, \overline{X} its closure, $\text{conv}(X)$ its convex hull, and 2^X its power-set. Moreover, for $\lambda \in \mathbb{R}$, the set $\lambda X := \{\lambda x : x \in X\}$. Given two subsets $X_a, X_b \subseteq X$, $d_H(X_a, X_b)$ denotes their Hausdorff distance (see [28]). Given an equivalence relation $Q \subseteq X \times X$, the set of all equivalence classes is denoted by X/Q . Finally, given a vector field $f : \mathbb{R}^n \rightarrow \mathbb{R}^n$ and a map $h : \mathbb{R}^n \rightarrow \mathbb{R}$, the Lie derivative of h along the flow of f , evaluated at a point $x \in \mathbb{R}^n$, is denoted by $\mathcal{L}_f h(x)$, i.e. $\mathcal{L}_f h(x) = \partial_x h(x) \cdot f(x)$. The k -th Lie derivative is defined as $\mathcal{L}_f^k h(x) = \mathcal{L}_f \mathcal{L}_f^{k-1} h(x)$, where $\mathcal{L}_f^0 h(x) = h(x)$.

Consider the system of ordinary differential equations (ODEs):

$$\dot{\zeta}(t) = f(\zeta(t)), \quad (1)$$

where $\zeta(t) \in \mathbb{R}^n$ and $f : \mathbb{R}^n \rightarrow \mathbb{R}^n$. A solution to system (1) with initial condition ζ_0 and initial time t_0 is denoted by $\zeta(t; t_0, \zeta_0)$. When t_0 (and ζ_0) is clear from the context, we omit it by writing $\zeta(t; \zeta_0)$ (respectively $\zeta(t)$). Given a set of initial states $\mathcal{I} \subseteq \mathbb{R}^n$, the *reachable set* of (1) at time T is defined as:

$$\mathcal{X}_T^f(\mathcal{I}) := \{\zeta(T; \zeta_0) : \zeta_0 \in \mathcal{I}\}.$$

Likewise, the *reachable flowpipe* of (1) in the time interval $[\tau_1, \tau_2]$, with initial set \mathcal{I} , is $\mathcal{X}_{[\tau_1, \tau_2]}^f(\mathcal{I}) :=$

$$\bigcup_{T \in [\tau_1, \tau_2]} \mathcal{X}_T^f(\mathcal{I}).$$

Now, consider the differential inclusion (DI):

$$\dot{\zeta}(t) \in F(\zeta(t)), \quad (2)$$

where $\zeta(t) \in \mathbb{R}^n$ and $F : \mathbb{R}^n \rightrightarrows \mathbb{R}^n$ is a set-valued map. Contrary to ODEs, which obtain unique solutions for each initial condition under mild assumptions, DIs generally obtain multiple solutions for each initial condition. We denote any solution of DI (2) with initial condition ζ_0 by $\zeta(t; \zeta_0)$ (we assume $t_0 = 0$ for ease of exposition). The set of all solutions of (2), which are defined in $[0, T]$, with initial condition in a set $\mathcal{I} \subseteq \mathbb{R}^n$, is denoted by $\mathcal{Z}_F([0, T]; \mathcal{I})$. Then, the *reachable set* of DI (2) from the initial set $\mathcal{I} \subseteq \mathbb{R}^n$ at time $T \geq 0$ is:

$$\mathcal{X}_T^F(\mathcal{I}) := \{\zeta(T) : \zeta \in \mathcal{Z}_F([0, T]; \mathcal{I})\}.$$

Moreover, the *reachable flowpipe* of DI (2) from the initial set $\mathcal{I} \subseteq \mathbb{R}^n$ within the time interval $[\tau_1, \tau_2]$ is $\mathcal{X}_{[\tau_1, \tau_2]}^F(\mathcal{I}) := \bigcup_{T \in [\tau_1, \tau_2]} \mathcal{X}_T^F(\mathcal{I})$. For more detail on differential inclusions, the reader is referred to [29].

2.2 Systems and Simulation Relations

Here we recall notions of systems and simulation relations from [30], which are employed later.

Definition 2.1 (System [30]). A system \mathcal{S} is a tuple $(X, X_0, U, \longrightarrow, Y, H)$, where X is the set of states, X_0 is the set of initial states, U is the set of inputs, $\longrightarrow \subseteq X \times U \times X$ is a transition relation, Y is the set of outputs and $H : X \rightarrow Y$ is the output map.

If X is a finite (or infinite) set, then \mathcal{S} is called finite-state (respectively infinite-state). A system \mathcal{S} is called a *metric system* if Y is equipped with a metric $d : Y \times Y \rightarrow \mathbb{R}_0^+ \cup \{+\infty\}$.

Definition 2.2 (ϵ -Approximate Simulation Relation [30]). Consider two metric systems $\mathcal{S}_a, \mathcal{S}_b$ with $Y_a = Y_b$ and a constant $\epsilon \geq 0$. A relation $Q \subseteq X_a \times X_b$ is an ϵ -approximate simulation relation from \mathcal{S}_a to \mathcal{S}_b if it satisfies:

- $\forall x_{0_a} \in X_{0_a} : \exists x_{0_b} \in X_{0_b}$ such that $(x_{0_a}, x_{0_b}) \in Q$,
- $\forall (x_a, x_b) \in Q : d(H_a(x_a), H_b(x_b)) \leq \epsilon$,
- $\forall x_a \in X_a$ with $(x_a, u_a, x'_a) \in \xrightarrow{a}$: if $(x_a, x_b) \in Q$ then $\exists (x_b, u_b, x'_b) \in \xrightarrow{b}$ such that $(x'_a, x'_b) \in Q$.

If there exists an ϵ -approximate simulation relation from \mathcal{S}_a to \mathcal{S}_b , we say that \mathcal{S}_b ϵ -approximately simulates \mathcal{S}_a and write $\mathcal{S}_a \stackrel{\epsilon}{\preceq} \mathcal{S}_b$. Moreover, let us introduce an alternative definition of *power quotient systems*. For the original definition, see [30].

Definition 2.3 (Power Quotient System [22]). Consider a system $\mathcal{S} = (X, X_0, U, \longrightarrow, Y, H)$ and an equivalence relation $Q \subseteq X \times X$. The power quotient system of \mathcal{S} is the tuple $\mathcal{S}_{/Q} = (X_{/Q}, X_{0/Q}, U_{/Q}, \xrightarrow{/Q}, Y_{/Q}, H_{/Q})$, where:

- $X_{/Q} = X/Q$,
- $X_{0/Q} = \{x_{/Q} \in X_{/Q} : x_{/Q} \cap X_0 \neq \emptyset\}$,
- $U_{/Q} = U$,
- $(x_{/Q}, u, x'_{/Q}) \in \xrightarrow{/Q}$ if $\exists (x, u, x')$ such that $x \in x_{/Q}$ and $x' \in x'_{/Q}$,
- $Y_{/Q} \subseteq 2^Y$,
- $H_{/Q}(x_{/Q}) = \bigcup_{x \in x_{/Q}} H(x)$.

Lemma 2.1 ([22]). Consider a metric system \mathcal{S} , an equivalence relation $Q \subseteq X \times X$ and the power quotient system $\mathcal{S}_{/Q}$. For any ϵ such that $\epsilon \geq \sup_{x \in x_{/Q}, x'_{/Q} \in X_{/Q}} d_H(H(x), H_{/Q}(x_{/Q}))$, $\mathcal{S}_{/Q}$

ϵ -approximately simulates \mathcal{S} , i.e. $\mathcal{S} \stackrel{\epsilon}{\preceq} \mathcal{S}_{/Q}$.

2.3 Homogeneous Systems and Differential Inclusions

In this work, we make use of certain properties of homogeneous systems and DIs. For our purposes, it suffices to consider the classical notion of homogeneity. For the general geometric definition and more information, the reader is referred to [31] and [32].

Definition 2.4 (Homogeneous functions and set-valued maps). Consider a function $f : \mathbb{R}^n \rightarrow \mathbb{R}^m$ (or a set-valued map $F : \mathbb{R}^n \rightrightarrows \mathbb{R}^m$). We say that f (or F) is homogeneous of degree $\alpha \in \mathbb{R}$, if for all $x \in \mathbb{R}^n$ and any $\lambda > 0$: $f(\lambda x) = \lambda^{\alpha+1} f(x)$ (respectively $F(\lambda x) = \lambda^{\alpha+1} F(x)$).

A dynamical system (1) (or a DI (2)) is called homogeneous of degree $\alpha \in \mathbb{R}$ if f (respectively F) is homogeneous of the same degree. Homogeneous systems and DIs possess the following important scaling property of solutions:

Proposition 2.1 (Scaling Property [31,32]). *Let the system of ODEs (1) be homogeneous of degree $\alpha \in \mathbb{R}$. Then, for any $\zeta_0 \in \mathbb{R}^n$ and any $\lambda > 0$:*

$$\zeta(t; \lambda\zeta_0) = \lambda\zeta(\lambda^\alpha t; \zeta_0). \quad (3)$$

Now, let DI (2) be homogeneous of degree $\alpha \in \mathbb{R}$. Then, for any $\mathcal{I} \subseteq \mathbb{R}^n$ and any $\lambda > 0$:

$$\mathcal{X}_t^F(\lambda\mathcal{I}) = \lambda\mathcal{X}_{\lambda^\alpha t}^F(\mathcal{I}). \quad (4)$$

2.4 Event-Triggered Control Systems

Consider the following control system with state feedback:

$$\dot{\zeta}(t) = f\left(\zeta(t), v(\zeta(t))\right), \quad (5)$$

where $\zeta : \mathbb{R}_0^+ \rightarrow \mathbb{R}^n$, $f : \mathbb{R}^n \rightarrow \mathbb{R}^n$ and $v : \mathbb{R}^n \rightarrow \mathbb{R}^m$. In a sample-and-hold digital implementation of (5), the input is held constant between consecutive *sampling time instants* t_i and is only updated at sampling times, i.e.:

$$\dot{\zeta}(t) = f\left(\zeta(t), v(\zeta(t_i))\right), \quad t \in [t_i, t_{i+1}). \quad (6)$$

The so-called *measurement error* is the deviation of the current state of (6) from the last measurement:

$$\varepsilon_\zeta(t) = \zeta(t) - \zeta(t_i), \quad t \in [t_i, t_{i+1}). \quad (7)$$

Observe that $\varepsilon_\zeta(t)$ resets to zero, at each sampling time t_i . By employing $\varepsilon_\zeta(t)$, we can write (6) as:

$$\dot{\zeta}(t) = f\left(\zeta(t), v(\zeta(t) + \varepsilon_\zeta(t))\right), \quad t \in [t_i, t_{i+1}). \quad (8)$$

In ETC, the sampling times are defined as follows:

$$t_{i+1} = t_i + \inf\{t > 0 : \phi(\zeta(t; x_i), \varepsilon_\zeta(t)) \geq 0\} \quad (9)$$

and $t_0 = 0$, where $x_i = \zeta(t_i)$ is the last state measurement, $\phi(\cdot, \cdot)$ is the *triggering function* and (9) is called *triggering condition*. The difference $t_{i+1} - t_i$ is called *inter-sampling time*. Each point $x \in \mathbb{R}^n$ in the state-space is associated to a unique inter-sampling time $\tau(x)$:

$$\tau(x) := \inf\{t > 0 : \phi(\zeta(t; x), \varepsilon_\zeta(t)) \geq 0\}. \quad (10)$$

Typically, the triggering function ϕ is designed such that the ETC sampling scheme (9) guarantees certain performance specifications (e.g. stability, boundedness, etc.). In other words, the satisfaction of $\phi(\zeta(t), \varepsilon_\zeta(t)) \leq 0$ for all $t \geq 0$ implies corresponding performance guarantees. The triggering function, between two sampling times t_i and t_{i+1} , starts from a negative value $\phi(\zeta(t_i), 0) < 0$ (the measurement error is zero at sampling times) and remains negative until it becomes zero at t_{i+1} , when the state is sampled again, the measurement error resets to zero, the triggering function resets to a negative value and the control action is updated.

By observing that $\dot{\varepsilon}_\zeta(t) = -\dot{\zeta}(t)$, we write the dynamics of the ETC system in the following extended form:

$$\begin{aligned} \dot{\xi}(t) &= \begin{bmatrix} f(\zeta(t), v(\zeta(t) + \varepsilon_\zeta(t))) \\ -f(\zeta(t), v(\zeta(t) + \varepsilon_\zeta(t))) \end{bmatrix} =: f_e(\xi(t)), \quad t \in [t_i, t_{i+1}) \\ \xi(t_{i+1}^+) &= [\zeta^\top(t_{i+1}^+) \quad 0^\top]^\top, \end{aligned} \quad (11)$$

where $\xi = (\zeta, \varepsilon_\zeta) \in \mathbb{R}^{2n}$. At each sampling time t_i , the state of (11) becomes $\xi_i = (x_i, 0)$. Thus, since we focus on intervals between consecutive sampling times $[t_i, t_{i+1})$, instead of writing $\phi(\xi(t; (x_i, 0)))$ (or $\tau((x_i, 0))$), we abusively write $\phi(\xi(t; x_i))$ (or $\tau(x_i)$) for convenience.

Finally, owing to the scaling property of solutions (see Proposition 2.1), the inter-sampling times of homogeneous ETC systems (11) with homogeneous triggering functions scale along *homogeneous rays* (straight lines that start from the origin and extend to infinity) as follows:

Theorem 2.2 (Scaling Law [11]). *Let the ETC system (11) be homogeneous of degree $\alpha \in \mathbb{R}$ (i.e. $f_e(\cdot)$ is homogeneous of degree α). Let the triggering function ϕ be homogeneous of degree $\theta \in \mathbb{R}$. For all $x \in \mathbb{R}^n$, the inter-sampling times $\tau(\cdot)$ defined by (10) scale according to:*

$$\tau(\lambda x) = \lambda^{-\alpha} \tau(x), \quad \lambda > 0. \quad (12)$$

The scaling law (12) will prove crucial in our construction of our abstraction later on.

3 Problem Statement: Nonlinear Systems without Disturbances and Uncertainties

In this work, we construct traffic abstractions of nonlinear ETC systems with disturbances, uncertainties and general triggering functions. For ease of presentation, we start by considering the case of systems without disturbances or uncertainties. Afterwards, we show how the proposed methodology can be adjusted such that it addresses perturbed uncertain systems, by employing tools developed in [13].

Consider the ETC system (8)-(9) (and its extended form (11)). We adopt a problem formulation similar to the one of [22, 26]. Let us introduce the system:

$$\mathcal{S} = (X, X_0, U, \longrightarrow, Y, H), \quad (13)$$

where $X = X_0 \subseteq \mathbb{R}^n$, U is a singleton (i.e. the system is autonomous), $Y \subseteq \mathbb{R}^+$, $H(x) = \tau(x)$ (where $\tau(\cdot)$ is defined in (10)) and the transition relation $\longrightarrow \subseteq X \times X$ is defined such that $(x, x') \in \longrightarrow \iff \zeta(\tau(x); x) = x'$, where we omit the input in the transition notation since the system is autonomous. The set of output sequences of system (13) is composed of all possible inter-sampling time sequences of the ETC system (8)-(9) to be abstracted; that is, system (13) captures exactly the traffic generated by the ETC system. However, it is infinite-state and cannot serve as a finite abstraction that can be computationally handled for traffic scheduling.

We, also, introduce the following set of assumptions:

Assumption 1.

1. The triggering function $\phi(\xi(t; x))$ is p -times continuously differentiable, where $p \geq 1$.

2. The vector field $f_e(\cdot)$ of the extended ETC system (11) is $p-1$ -times continuously differentiable (with $p \geq 1$) and locally bounded.
3. For all $\xi_0 = (x_0, 0) \in \mathbb{R}^{2n}$: $\phi(\xi_0) < 0$. Moreover, for any compact set $K \subset \mathbb{R}^n$ there exists $\epsilon_K > 0$ such that for all $x_0 \in K$, $\phi(\xi(t; x_0)) < 0$ for all $t \in [0, \epsilon_K)$.
4. The set X is a connected bounded polytope, i.e. the system operates in a bounded connected polytope of \mathbb{R}^n , and $0 \in \text{int}(X)$.

Assumption 1 includes a wide class of systems and triggering functions. In particular, it suffices that f_e is continuous and that ϕ satisfies items 1 and 3, which are satisfied by most triggering functions in the ETC literature (e.g. Lebesgue sampling [1], Mixed-Triggering [6]). Item 3 serves to impose that the given ETC system does not exhibit infinitely fast sampling (Zeno behaviour). Finally, item 4 could be relaxed to X being just connected and bounded, but we assume that it is a polytope and $0 \in \text{int}(X)$ for ease of presentation.

Remark 1. The triggering function proposed in [4] does not satisfy item 3, as $\phi(\xi(0; 0)) = 0$. Due to this fact, for arbitrarily small disturbances, it leads to infinitely fast sampling (Zeno behaviour) when the system is close to the origin. That is the reason why we rule it out. Nevertheless, as commented later in the document, the case of ETC systems with the triggering function of [4] (without disturbances or uncertainties) can indeed be addressed by our proposed methodology.

Since system (13) captures exactly the timing behavior of the ETC system (8)-(9), abstracting the ETC system is equivalent to abstracting system (13). This gives rise to the following problem statement:

Problem Statement 1. Consider the infinite-state system \mathcal{S} (13). Let Assumption 1 hold. Construct an equivalence relation $Q \subseteq X \times X$ and a power quotient system $\mathcal{S}/Q = (X/Q, X_{0/Q}, U/Q, \xrightarrow{/Q}, Y/Q, H/Q)$ with:

- $X/Q = X/Q := \{\mathcal{R}_1, \dots, \mathcal{R}_i, \dots, \mathcal{R}_q\}$,
- $X_{0/Q} = \{\mathcal{R}_i : \mathcal{R}_i \cap X_0 \neq \emptyset\} = X/Q$,
- $U/Q = U$,
- $(x/Q, x'/Q) \in \xrightarrow{/Q}$ if $\exists x \in x/Q$ and $\exists x' \in x'/Q$ such that $\zeta(H(x); x) = x'$,
- $Y/Q \subseteq 2^Y = 2^{\mathbb{R}^+}$,
- $H/Q(\mathcal{R}_i) := [\underline{\tau}_i, \bar{\tau}_i]$, with:

$$\underline{\tau}_i \leq \inf_{x \in \mathcal{R}_i} H(x), \quad \bar{\tau}_i \geq \sup_{x \in \mathcal{R}_i} H(x). \quad (14)$$

First, note that the states of the quotient system are regions in the state-space of the ETC system, i.e. $\mathcal{R}_i \subseteq X \subset \mathbb{R}^n$. A transition from \mathcal{R}_i to \mathcal{R}_j is defined if there exists a trajectory starting from $x \in \mathcal{R}_i$, which lies in \mathcal{R}_j at the inter-sampling time $\tau(x)$. Hence, a transition is taken every time the triggering condition (9) is satisfied. Finally, eq. (14) indicates that the quotient system's output of a region \mathcal{R}_i is an interval that contains all possible inter-sampling times that correspond to all states $x \in \mathcal{R}_i$. Thus, given any run of the ETC system and a corresponding run of the abstraction, the abstraction's output sequence is a sequence of intervals, each of which containing the inter-sampling time that the ETC system exhibited at that particular step of the run. In fact, by employing Lemma 2.1, we can conclude that $\mathcal{S} \stackrel{\epsilon}{\preceq} \mathcal{S}/Q$, for all $\epsilon \geq \max_i \{\bar{\tau}_i - \underline{\tau}_i\}$.

4 Homogenized ETC Systems and Inner-Approximations of Isochronous Manifolds

To abstract nonlinear ETC systems (8)-(9), and especially to determine lower bounds $\underline{\tau}_i$ on inter-sampling times $\tau(x)$ for the regions \mathcal{R}_i , we make use of theoretical tools such as the scaling law (12), the homogenization procedure [27] and approximations of isochronous manifolds [12, 13]. In this section, we recall these notions and show how they enable determining lower bounds of ETC inter-sampling times.

4.1 Homogenization Procedure

According to the homogenization procedure proposed in [27], the extended ETC system (11) is rendered homogeneous of degree $\alpha > 0$ by adding a dummy variable w as follows:

$$\begin{bmatrix} \dot{\xi} \\ \dot{w} \end{bmatrix} = \begin{bmatrix} w^{\alpha+1} f_e(w^{-1}\xi) \\ 0 \end{bmatrix} = \tilde{f}_e(\xi, w) \quad (15)$$

Moreover, a triggering function ϕ is rendered homogeneous of degree $\theta > 0$ in the same way:

$$\tilde{\phi}(\xi, w) = w^{\theta+1} \phi(w^{-1}\xi) \quad (16)$$

For the remaining, we denote inter-sampling times of points $(x, w) \in \mathbb{R}^{n+1}$ produced by the homogenized ETC system (15)-(16) by $\tilde{\tau}((x, w))$ (recall that we abusively use the notation $\tilde{\tau}((x, w))$ instead of $\tilde{\tau}((x, 0, w))$). As discussed in [27], since the ξ -trajectories of the homogenized system (15)-(16) with initial condition $(x_0, e_0, 1) \in \mathbb{R}^{2n+1}$ coincide with the trajectories of the initial ETC system (11) with initial condition $(x_0, e_0) \in \mathbb{R}^{2n}$, for all $x_0 \in \mathbb{R}^n$ we have:

$$\tilde{\tau}((x_0, 1)) = \tau(x_0), \quad (17)$$

where $\tau(x_0)$ is the inter-sampling time produced by the original ETC system (11) with triggering function ϕ corresponding to the point $x_0 \in \mathbb{R}^n$. Finally, since (15) is homogeneous of degree α , the inter-sampling times $\tilde{\tau}((x, w))$ follow the scaling law (12): $\tilde{\tau}(\lambda(x, w)) = \lambda^{-\alpha} \tilde{\tau}((x, w))$.

4.2 Inner-Approximations of Isochronous Manifolds

Let us recall the notion of isochronous manifolds introduced in [27], and the methodology that derives inner-approximations of isochronous manifolds, from [12] and [13].

Definition 4.1 (Isochronous Manifold). *Consider an ETC system (8)-(9). The set $M_{\tau_*} = \{x \in \mathbb{R}^n : \tau(x) = \tau_*\}$, where $\tau(x)$ is as in (10), is called isochronous manifold of time τ_* .*

To obtain actual isochronous manifolds, one would need a closed-form solution of the (generally nonlinear) ETC system, which is most often impossible to obtain. Thus, in [12] and [13], we developed a method that derives analytical expressions of *inner-approximations* \underline{M}_{τ_*} of isochronous manifolds.

To derive approximations of isochronous manifolds, the system and the triggering function are both rendered homogeneous, via the homogenization procedure. Let $Z \subset \mathbb{R}^n$ be compact and

connected with $0 \in \text{int}(Z)$, consider the set $W = [\underline{w}, \bar{w}]$ with $\bar{w} > \underline{w} > 0$, and define the following sets:

$$\begin{aligned}\Phi &:= \bigcup_{x_0 \in Z} \{x \in \mathbb{R}^n : e = x_0 - x, w \in W, \tilde{\phi}((x, e, w)) \leq 0\}, \\ E &:= \{x_0 - x \in \mathbb{R}^n : x_0 \in Z, x \in \Phi\}, \\ \Xi &:= \Phi \times E \times W,\end{aligned}\tag{18}$$

where $\tilde{\phi}$ is the homogenized triggering function (16). For the remaining, we introduce the following assumption:

Assumption 2. *The set $\Phi \subset \mathbb{R}^n$ is compact.*

This assumption is satisfied by most known triggering functions ϕ (e.g. Lebesgue sampling [1], Tabuada's triggering function [4], Mixed-Trigging [6], etc.). The following theorem provides a method to construct sets that inner-approximate isochronous manifolds of a homogenized ETC system (15) inside a cone \mathcal{C} :

Theorem 4.1 ([12, 13]). *Consider the homogenized ETC system (15) - (16), the sets Z, W, Φ, E, Ξ defined in (18) and let Assumptions 1 and 2 hold. Let $\delta_0, \dots, \delta_p \geq 0$ be such that:*

$$\mathcal{L}_{\tilde{f}_e}^p \tilde{\phi}((z, w)) \leq \sum_{i=0}^{p-1} \delta_i \mathcal{L}_{\tilde{f}_e}^i \tilde{\phi}((z, w)) + \delta_p, \quad \forall (z, w) \in \Xi,\tag{19a}$$

$$\delta_0 \tilde{\phi}((z, w)) + \delta_p \geq c > 0, \quad \forall (z, w) \in Z \times \{0\} \times W,\tag{19b}$$

where $c > 0$ is an arbitrary positive constant. Let $\rho > \underline{w}$ be such that $D_\rho := \{(x, w) \in \mathbb{R}^{n+1} : |(x, w)| = \rho, w \in W\} \subset Z \times W$. For all $(x, w) \in \mathbb{R}^{n+1} \setminus \{0\}$ define the function:

$$\mu((x, w), t) := \left(\frac{|(x, w)|}{\rho}\right)^{\theta+1} C e^{A \left(\frac{|(x, w)|}{\rho}\right)^\alpha t} \mu_0,\tag{20}$$

where:

$$A = \begin{bmatrix} 0 & 1 & 0 & \dots & 0 & 0 \\ 0 & 0 & 1 & \dots & 0 & 0 \\ \vdots & \vdots & & \ddots & \vdots & \vdots \\ 0 & 0 & 0 & \dots & 1 & 0 \\ \delta_0 & \delta_1 & \delta_2 & \dots & \delta_{p-1} & 1 \\ 0 & 0 & 0 & \dots & 0 & 0 \end{bmatrix}, \quad C = \begin{bmatrix} 1 \\ 0 \\ \vdots \\ 0 \end{bmatrix}^\top, \quad \mu_0 = \begin{bmatrix} \phi\left(\left(\rho \frac{x}{|(x, w)|}, 0, \rho \frac{w}{|(x, w)|}\right)\right) \\ \max\left(\mathcal{L}_f \phi\left(\left(\rho \frac{x}{|(x, w)|}, 0, \rho \frac{w}{|(x, w)|}\right)\right), 0\right) \\ \vdots \\ \max\left(\mathcal{L}_f^{p-1} \phi\left(\left(\rho \frac{x}{|(x, w)|}, 0, \rho \frac{w}{|(x, w)|}\right)\right), 0\right) \\ \delta_p \end{bmatrix}$$

and α, θ are the degrees of homogeneity of the system and the triggering function, respectively. The sets

$$\underline{M}_{\tau_\star} = \{(x, w) \in \mathbb{R}^{n+1} : \mu((x, w), \tau_\star) = 0\}\tag{21}$$

are hypersurfaces of dimension n encircling the origin and inner-approximate isochronous manifolds M_{τ_\star} of the homogenized system (15) inside the cone:

$$\mathcal{C} = \{(x, w) \in \mathbb{R}^n \times \mathbb{R}_+ : |x|^2 + w^2 \leq \frac{w^2}{\underline{w}^2} \rho^2\} \setminus \{0\},\tag{22}$$

i.e. for all $(x, w) \in \underline{M}_{\tau_\star} \cap \mathcal{C}$:

- $\exists! \kappa_{(x,w)} \geq 1$ s.t. $\kappa_{(x,w)}(x, w) \in M_{\tau_\star}$
- $\exists \lambda_{(x,w)} \in (0, 1)$ s.t. $\lambda_{(x,w)}(x, w) \in \underline{M}_{\tau_\star}$.

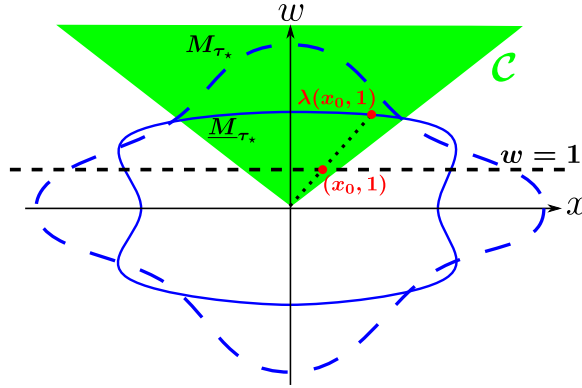


Figure 1: Approximation $\underline{M}_{\tau_\star}$ (solid blue line) of an isochronous manifold M_{τ_\star} (dashed blue line). Inside the cone \mathcal{C} (green cone), the set $\underline{M}_{\tau_\star}$ inner-approximates M_{τ_\star} . For the point $(x_0, 1) \in \mathcal{C}$ on the $w = 1$ -hyperplane, there exists $\lambda > 0$ such that $\lambda(x_0, 1) \in \underline{M}_{\tau_\star} \cap \mathcal{C}$. For this point, $\tilde{\tau}((x_0, 1)) \geq \lambda^\alpha \tau_\star$.

The core idea of Theorem 4.1 is constructing a function μ , which a) upper-bounds the triggering function $\tilde{\phi}$ for initial conditions $(x_0, w_0) \in \mathcal{C}$, b) starts from a negative value (observe that $\mu((x_0, w_0), 0) = \tilde{\phi}(\xi(x_0; 0), w(w_0; 0)) < 0$), and c) obtains only one zero-crossing w.r.t. time. Thus, by the scaling law (12), the zero-level sets $\underline{M}_{\tau_\star}$ of μ inner-approximate the isochronous manifolds M_{τ_\star} inside the cone \mathcal{C} . For more information, the reader is referred to [12, 13]. An approximation $\underline{M}_{\tau_\star}$ of an isochronous manifold M_{τ_\star} is depicted in Figure 1. Observe that inside the cone \mathcal{C} (22), the set $\underline{M}_{\tau_\star}$ inner-approximates M_{τ_\star} (it is closer to the origin, in every direction inside the cone).

Remark 2. As discussed in [12] and [13], under Assumptions 1 and 2, coefficients $\delta_i \geq 0$ that satisfy (19) always exist; e.g. $\delta_0, \dots, \delta_{p-1} = 0$ and $\delta_p \geq \max\left\{c, \sup_{(z,w) \in \Xi} \mathcal{L}_{\tilde{f}_e}^p \tilde{\phi}((z, w))\right\}$. In [12], a computational algorithm has been proposed, that computes the coefficients δ_i , by using Linear Programming and Satisfiability-Modulo Theory solvers (SMT, see e.g. [33]).

4.3 Lower Bounds on ETC Inter-Sampling Times

Obtaining approximations of isochronous manifolds of the homogenized ETC system allows to determine lower bounds on inter-sampling times of the original ETC system:

Proposition 4.1. Consider the ETC system (8)-(9), its extended form (11), and the homogenized one (15)-(16). Let Assumptions 1 and 2 hold. Let $\underline{M}_{\tau_\star}$ be an approximation of isochronous manifold M_{τ_\star} of the homogenized system, derived as dictated in Theorem 4.1. Consider a point $(x_0, 1) \in \mathcal{C}$. Then, there exists a $\lambda > 0$ such that $\lambda(x_0, 1) \in \underline{M}_{\tau_\star}$. Moreover, the inter-sampling time $\tau(x_0)$ produced by the original ETC system (8)-(9) is lower-bounded as follows:

$$\tau(x_0) \geq \lambda^\alpha \tau_\star \quad (23)$$

Proof. See Appendix. □

To obtain the lower bound $\lambda^\alpha \tau_\star$ on the inter-sampling time $\tau(x_0)$, what remains is to compute the *scaling factor* $\lambda > 0$ (or a lower bound of λ). This is addressed in the next section, and used to finally determine lower-bounds $\underline{\tau}_i$ on the inter-sampling times of regions \mathcal{R}_i .

Remark 3. *As discussed in [13], due to the fact that inner-approximations are valid only in the cone \mathcal{C} (22), Proposition 4.1 is able to determine lower bounds on inter-sampling times only for points belonging in the ball $B := \{x_0 \in \mathbb{R}^n : |x_0|^2 \leq \frac{\rho^2 - \underline{w}^2}{\underline{w}^2}\}$, where $\underline{w} > 0$ is given in the definition of the set W above equation (18), and $\rho > \underline{w}$ is given in Theorem 4.1. Since we can freely select \underline{w} to be arbitrarily small, without changing ρ , the set B can be selected arbitrarily large. Thus, by selecting B such that $X \subseteq B$, we can determine lower bounds on inter-sampling times for all regions \mathcal{R}_i .*

5 Abstracting Nonlinear Systems without Disturbances and Uncertainties

In this section, we address Problem Statement 1. The state-space $X \subset \mathbb{R}^n$ is partitioned into a finite number of polytopes $\{\mathcal{R}_1, \dots, \mathcal{R}_q\}$, thus determining the relation Q the abstraction's state set X/Q . To obtain lower bounds $\underline{\tau}_i$ on inter-sampling times $\tau(x)$ for regions \mathcal{R}_i , we homogenize the ETC system and the triggering function using the homogenization procedure (15)-(16). Afterwards, given an approximation $\underline{M}_{\tau_\star}$ of isochronous manifolds of the homogenized system, we calculate a lower bound λ_i on the minimum scaling factor between points in \mathcal{R}_i (which is represented by a subset of the $w = 1$ -hyperplane of \mathbb{R}^{n+1}) and the approximation. The lower-bounds $\underline{\tau}_i$ are then obtained by using λ_i along with the scaling law (12) (as shown in Proposition 4.1). Finally, the upper-bounds $\bar{\tau}_i$ and the transitions from regions \mathcal{R}_i to regions \mathcal{R}_j are determined simultaneously, by employing reachability analysis, in a way similar to [26].

5.1 State-Space Partition and Determination of Lower Bounds on Inter-Sampling Times

The state-space of the original ETC system (8)-(9) is partitioned into a finite number of polytopes \mathcal{R}_i . Let the origin be solely contained in the region \mathcal{R}_{q_0} . We assume that the polytopes \mathcal{R}_i are given in vertex representation:

$$\mathcal{R}_i = \text{conv}\left(\{x_{i_1}, \dots, x_{i_{2^n}}\}\right), \quad (24)$$

where $\{x_{i_1}, \dots, x_{i_{2^n}}\}$ is the set of extreme vertices of \mathcal{R}_i . Hence, the equivalence relation Q is designed as follows:

$$Q := \{(x, y) \in \mathbb{R}^n \times \mathbb{R}^n : x \in \mathcal{R}_i \iff y \in \mathcal{R}_i, i = 1, \dots, q\}.$$

To determine lower bounds $\underline{\tau}_i$ on inter-sampling times of regions \mathcal{R}_i we make use of Proposition 4.1. Thus, the ETC system and the triggering function are homogenized via the homogenization procedure (15)-(16). The state-space $X \subset \mathbb{R}^n$ of the original ETC system (8)-(9) is mapped to the $w = 1$ -hyperplane of \mathbb{R}^{n+1} (see Figure 3) and the regions \mathcal{R}_i are, then, represented by n -dimensional polytopes lying on the $w = 1$ -hyperplane of \mathbb{R}^{n+1} . To avoid confusion, we denote these polytopes by

$$\tilde{\mathcal{R}}_i := \{(x, 1) \in \mathbb{R}^{n+1} : x \in \mathcal{R}_i\} \quad (25)$$

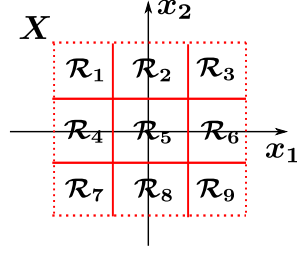


Figure 2: Partition of the state space X (dashed box) of a 2-dimensional ETC system into 9 polytopes \mathcal{R}_i (with $q_0 = 5$).

Moreover, we denote the polyhedral cone pointed at the origin and delimited by the vertices of $\tilde{\mathcal{R}}_i$ by:

$$\mathcal{C}_i := \{y \in \mathbb{R}^{n+1} : y = \sum_{j=1}^{2^n} \alpha_j \cdot (x_{i_j}, 1), \alpha_j \geq 0, j = 1, \dots, 2^n\} \quad (26)$$

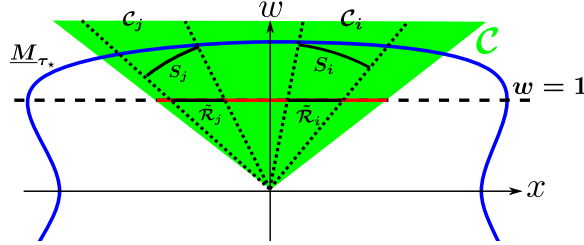


Figure 3: Embedding of the ETC system (8)-(9) in \mathbb{R}^{n+1} . Its state space X is mapped to the red segment of the $w = 1$ -hyperplane. The regions $\mathcal{R}_i \subset \mathbb{R}^n$ are represented by polytopes $\tilde{\mathcal{R}}_i \subset \mathbb{R}^{n+1}$ lying on $w = 1$. The sets \mathcal{C}_i are cones pointed at the origin with their extreme rays passing through the vertices of $\tilde{\mathcal{R}}_i$. Each conic section $\underline{M}_{\tau_*} \cap \mathcal{C}_i$ of the approximation \underline{M}_{τ_*} (blue curve) of isochronous manifold M_{τ_*} is inner-approximated by spherical segments S_i .

Directly from (17), we have that the lower bound on inter-sampling times of region $\tilde{\mathcal{R}}_i$ coincides with the lower bound on the ones of region \mathcal{R}_i . As shown in Proposition 4.1, given an approximation \underline{M}_{τ_*} of an isochronous manifold, to determine a lower bound for inter-sampling times of $\tilde{\mathcal{R}}_i$, we have to find (a lower bound on) *the smallest* λ for which: $\exists(x_0, 1) \in \tilde{\mathcal{R}}_i$ such that $\lambda(x_0, 1) \in \underline{M}_{\tau_*}$. Computationally, this is a very challenging problem, as the representation of \underline{M}_{τ_*} is transcendental. To alleviate it, we inner-approximate the conic intersection $\underline{M}_{\tau_*} \cap \mathcal{C}_i$ by a spherical segment S_i (see Figure 3), where $S_i := \{y \in \mathcal{C}_i : |y| = r_i\}$. Then, given S_i , the timing lower-bound for \mathcal{R}_i can be computed as follows:

Proposition 5.1. *Consider the ETC system (8)-(9), its extended form (11), and the homogenized system and triggering function (15)-(16). Let Assumptions 1 and 2 hold. Let \underline{M}_{τ_*} be an approximation of isochronous manifold M_{τ_*} of (15)-(16). Let $\mathcal{R}_i \subset X$ be given in (24). Consider the polyhedral cone $\mathcal{C}_i \subset \mathbb{R}^{n+1}$ defined in (26). Let the spherical segment:*

$$S_i := \{y \in \mathcal{C}_i : |y| = r_i\}, \quad (27)$$

with $r_i > 0$, be an inner approximation of $\underline{M}_{\tau_\star} \cap \mathcal{C}_i$, i.e.:

$$\forall y \in S_i : \exists! \lambda_y \geq 1 \text{ such that } \lambda_y y \in \underline{M}_{\tau_\star} \cap \mathcal{C}_i.$$

Let $(x_{i_\star}, 1) \in \tilde{\mathcal{R}}_i$ be the maximum-Euclidean-norm element of $\tilde{\mathcal{R}}_i$, i.e.:

$$(x_{i_\star}, 1) := \arg \max_{(x,1) \in \tilde{\mathcal{R}}_i} |(x,1)|. \quad (28)$$

Then, the inter-sampling times of all points in \mathcal{R}_i (produced by system (8)-(9)) are lower bounded as:

$$\forall x \in \mathcal{R}_i : \tau(x) \geq \left(\frac{r_i}{|(x_{i_\star}, 1)|} \right)^\alpha \tau_\star =: \underline{\tau}_i. \quad (29)$$

Proof. See Appendix. □

Remark 4. When the ETC system (11) is already homogeneous, it is redundant to further homogenize it. In such case, the w -variable is dropped from all our derivations, and the approximations of isochronous manifolds can be derived in the original state space \mathbb{R}^n (in Theorem 4.1 we replace $Z \times W$ with only Z , see [12] for more information), where the scaling law holds. Afterwards, the same procedure can be followed, in order to determine the lower bounds $\underline{\tau}_i$. Finally, even though in [26] a different way of partitioning the state-space of homogeneous ETC systems and deriving the lower bounds has been proposed, the methodology presented here is applicable to general nonlinear systems, thus including homogeneous ones as well. More discussion on that can be found in Section 8.

To determine $\underline{\tau}_i$, what remains is to find $(x_{i_\star}, 1)$ and the spherical segment S_i . Regarding the former, since $\tilde{\mathcal{R}}_i$ is a convex n -polytope, the maximum-norm element $(x_{i_\star}, 1)$ is one of its extreme vertices, and we can find it by comparing the extreme vertices' norms. To compute S_i , we employ the following proposition:

Proposition 5.2. The spherical segment $S_i := \{y \in \mathcal{C}_i : |y| = r_i\}$, where $r_i > 0$, inner-approximates $\underline{M}_{\tau_\star} \cap \mathcal{C}_i$ if:

$$\forall (x, w) \in S_i : \mu((x, w), \tau_\star) \leq 0. \quad (30)$$

Proof. See Appendix. □

As proposed in [26], one can find r_i that satisfies (30), by employing a line search and iteratively checking the satisfaction of (30) via an SMT (Satisfiability Modulo Theory) solver (e.g. [33]). To do that, first the halfspace representation of \mathcal{C}_i is obtained, which is more handleable by SMT solvers than the vertex one, via the double-description algorithm (see [34]). Although the worst-case complexity of this algorithm is known to be exponential in the size of the input and the output, certain heuristic modifications render it very competitive. Moreover, to avoid the numerically non-robust computations involving the symbolic (in terms of computational object) matrix exponential $e^{A \left(\frac{|(x, w)|}{\rho} \right)^\alpha \tau_\star}$ in (30), by observing that $(x, w) \in S_i \implies |(x, w)| = r_i$, we can fix $|(x, w)| \leftarrow r_i$, which transforms the previously symbolic matrix exponential into a regular numerical one. Thus, (30) becomes:

$$\forall (x, w) \in S_i : \left(\frac{r_i}{\rho} \right)^{\theta+1} C e^{A \left(\frac{r_i}{\rho} \right)^\alpha \tau_\star} \mu_0 \leq 0, \quad (31)$$

where A, C, μ_0 are given in Theorem 4.1. Then, r_i is obtained via a line search and iteratively checking (31). Finally, once r_i is computed, the timing lower-bound $\underline{\tau}_i$ for each region \mathcal{R}_i is determined as in Proposition 5.1.

5.2 Upper Bounds on Inter-Sampling Times and State Transitions

What remains is to determine the upper-bounds on inter-sampling times and the state transitions between the regions. The following proposition from [26] provides a condition that determines the timing upper bound $\bar{\tau}_i$ for each region \mathcal{R}_i :

Proposition 5.3 ([26]). *Consider the ETC system (8)-(9) and its extended form (11). Let Assumptions 1 and 2 hold. Let $\mathcal{R}_i \subseteq X$. Define the following sets:*

$$\begin{aligned}\mathcal{I}_i &:= \{(x, 0) \in \mathbb{R}^{2n} : x \in \mathcal{R}_i\} \\ \mathcal{U} &:= \{(x, e) \in \mathbb{R}^{2n} : \phi((x, e)) \leq 0\}\end{aligned}$$

If:

$$\mathcal{X}_{\tau_{i_{\max}}}^{f_e}(\mathcal{I}_i) \cap \mathcal{U} = \emptyset, \quad (32)$$

then for all $x \in \mathcal{R}_i$: $\tau(x) \leq \tau_{i_{\max}}$, where $\tau(\cdot)$ is as in (10).

Proof. If $\mathcal{X}_{\tau_{i_{\max}}}^{f_e}(\mathcal{I}_i) \cap \mathcal{U} = \emptyset$, then for all $x \in \mathcal{R}_i$ we have that $\phi(\xi(\tau_{i_{\max}}; x)) > 0$. Thus, $\tau(x) \leq \tau_{i_{\max}}$. \square

To provide an explanation of Proposition 5.3, satisfaction of (32) implies that ϕ , evaluated along any trajectory produced by the continuous dynamics of (11) (without the jumps at t_{i+1}) starting from \mathcal{I}_i , has already become positive at $\tau_{i_{\max}}$. Thus, $\tau_{i_{\max}}$ upper bounds inter-sampling times of all points in \mathcal{R}_i .

In order to check condition (32), we employ *reachability-analysis* computational tools (e.g. [24, 25]). Such tools, given a system (1), a set of initial conditions $\mathcal{I} \subset \mathbb{R}^n$ and a set $\mathcal{U} \subseteq \mathbb{R}^n$, by computing overapproximations of the reachable flowpipes $\mathcal{X}_{[\tau_1, \tau_2]}^f(\mathcal{I})$ and the set \mathcal{U} , they check if trajectories starting from \mathcal{I} enter \mathcal{U} , i.e. if $\mathcal{X}_{[\tau_1, \tau_2]}^f(\mathcal{I}) \cap \mathcal{U} = \emptyset$. We denote the corresponding overapproximations by $\hat{\mathcal{X}}_{[\tau_1, \tau_2]}^f(\mathcal{I})$, $\hat{\mathcal{U}}$, i.e. $\mathcal{X}_{[\tau_1, \tau_2]}^f(\mathcal{I}) \subseteq \hat{\mathcal{X}}_{[\tau_1, \tau_2]}^f(\mathcal{I})$ and $\mathcal{U} \subseteq \hat{\mathcal{U}}$. Thus, we have:

$$\hat{\mathcal{X}}_{[\tau_1, \tau_2]}^f(\mathcal{I}) \cap \hat{\mathcal{U}} = \emptyset \implies \mathcal{X}_{[\tau_1, \tau_2]}^f(\mathcal{I}) \cap \mathcal{U} = \emptyset, \quad (33)$$

Consequently, by employing a line search on $\tau_{i_{\max}}$, via a reachability analysis tool we can check iteratively if $\hat{\mathcal{X}}_{\tau_{i_{\max}}}^{f_e}(\mathcal{I}_i) \cap \hat{\mathcal{U}} = \emptyset$, until it is satisfied. The satisfaction of this equation implies the satisfaction of (32) (according to (33)), which in turn implies that $\tau(x) \leq \tau_{i_{\max}} = \bar{\tau}_i$ for all $x \in \mathcal{R}_i$, according to Proposition 5.3. This is how the upper bound $\bar{\tau}_i$ for each region \mathcal{R}_i is determined.

Now, let us use the computed flowpipes $\hat{\mathcal{X}}_{[\underline{\tau}_i, \bar{\tau}_i]}^{f_e}(\mathcal{I}_i)$ to derive the state transitions of the abstraction. First, observe that overapproximations $\hat{\mathcal{X}}_{[\underline{\tau}_i, \bar{\tau}_i]}^f(\mathcal{R}_i)$ of the reachable flowpipes of the ETC system (8) can be readily obtained by the already computed flowpipes $\hat{\mathcal{X}}_{[\underline{\tau}_i, \bar{\tau}_i]}^{f_e}(\mathcal{I}_i)$ of the extended system (11) as a projection to the ζ -variables:

$$\hat{\mathcal{X}}_{[\underline{\tau}_i, \bar{\tau}_i]}^f(\mathcal{R}_i) = \pi_{\zeta} \hat{\mathcal{X}}_{[\underline{\tau}_i, \bar{\tau}_i]}^{f_e}(\mathcal{I}_i).$$

Recall the transitions' definition, from Problem Statement 1:

$$(\mathcal{R}_i, \mathcal{R}_j) \in \xrightarrow{/Q}, \text{ if } : \quad \exists x \in \mathcal{R}_i \text{ and } \exists x' \in \mathcal{R}_j \text{ such that } \zeta(H(x); x) = x'.$$

This definition can be relaxed as follows:

$$(\mathcal{R}_i, \mathcal{R}_j) \in \xrightarrow{/Q}, \text{ if } : \quad \mathcal{X}_{[\underline{\tau}_i, \bar{\tau}_i]}^f(\mathcal{R}_i) \cap \mathcal{R}_j \neq \emptyset. \quad (34)$$

Thus, inspired by (33) and employing a reachability analysis tool, we can check if $\hat{\mathcal{X}}_{[\underline{\tau}_i, \bar{\tau}_i]}^f(\mathcal{R}_i) \cap \mathcal{R}_j \neq \emptyset$, which approximates condition (34) above, and if it is satisfied we define a transition $(\mathcal{R}_i, \mathcal{R}_j) \in \xrightarrow{/Q}$.

Remark 5. *In this way, the constructed abstraction contains all possible transitions $(\mathcal{R}_i, \mathcal{R}_j)$ defined as in (34). Notice that, since (34) is a relaxation of the original transitions' definition, and $\hat{\mathcal{X}}_{[\underline{\tau}_i, \bar{\tau}_i]}^f(\mathcal{R}_i) \cap \mathcal{R}_j \neq \emptyset$ does not necessarily imply that $\mathcal{X}_{[\underline{\tau}_i, \bar{\tau}_i]}^f(\mathcal{R}_i) \cap \mathcal{R}_j \neq \emptyset$, the abstraction may contain spurious transitions as well, i.e. transitions $(\mathcal{R}_i, \mathcal{R}_j)$ for which $\nexists x \in \mathcal{R}_i$ and $\nexists x' \in \mathcal{R}_j$ such that $\zeta(H(x); x) = x'$. However, the existence of spurious transitions does not affect the fact that $S_{/Q}$ ϵ -approximately simulates S (see [30]).*

Remark 6. *Assuming that the origin of the ETC system (8)-(9) is an equilibrium, its inter-sampling time $\tau(0) = +\infty$ (since $\phi(\xi(0; 0)) < 0$ and $\mathcal{L}_f^i \phi(0) = 0$). Hence, \mathcal{R}_{q_0} does not admit an upper bound on its inter-sampling times. In practice, to cope with that fact, an arbitrary maximum inter-sampling time τ_h is introduced (often called "heartbeat"), such that sampling instants are determined by $t_{i+1} = t_i + \min(\tau(x_i), \tau_h)$, where x_i is the last measured state and $\tau(\cdot)$ is defined in (10). Thus, for \mathcal{R}_{q_0} , we can arbitrarily dictate an upper bound $\bar{\tau}_{q_0} = \tau_h$ to be equal to the heartbeat, and force the sensors to sample according to $t_{i+1} = t_i + \min(\tau(x_i), \tau_h)$. Obviously, the heartbeat could be applied for any region \mathcal{R}_i , such that the upper bounds on their inter-sampling times could be defined as $\bar{\tau}_i = \min(\tau_{i_{\max}}, \tau_h)$, where $\tau_{i_{\max}}$ is the upper-bound as derived above.*

Remark 7. *When the triggering function considered is the one proposed by [4], the only modification to our technique needed concerns the lower bound on inter-sampling times of \mathcal{R}_{q_0} (assuming that the origin is the equilibrium). As discussed in [12], the proposed methodology is not able to derive a lower bound on inter-sampling times for \mathcal{R}_{q_0} in this case, since the approximations \underline{M}_{τ^*} obtain a singularity at the origin. In such case, we could select \mathcal{R}_{q_0} arbitrarily small, and then dictate a fixed inter-sampling time $\tau_h = \underline{\tau}_{q_0} = \bar{\tau}_{q_0}$ and force periodic sampling with period τ_h while the system lies in \mathcal{R}_{q_0} .*

6 Addressing Disturbances and Uncertainties

Here, we adjust the above methodology, to construct traffic abstractions of perturbed uncertain ETC systems. In particular, first we recall from [13] how ETC systems with uncertainties/disturbances are modelled as DIs, and adjust Problem Statement 1 such that it considers perturbed uncertain systems. Afterwards, we address the new problem statement by employing the extensions of results such as the homogenization procedure, the scaling law and approximations of isochronous manifolds to perturbed uncertain systems, derived in [13].

6.1 Perturbed Uncertain ETC Systems and Differential Inclusions

We consider perturbed uncertain ETC systems, written as:

$$\begin{aligned}\dot{\zeta}(t) &= f\left(\zeta(t), v(\zeta(t) + \varepsilon_\zeta(t)), d(t)\right), \quad t \in [t_i, t_{i+1}), \\ t_{i+1} &= t_i + \inf\{t > 0 : \phi(\zeta(t; x_i), \varepsilon_\zeta(t)) \geq 0\}.\end{aligned}\tag{35}$$

where $d : \mathbb{R}_0^+ \rightarrow \mathbb{R}^{m_d}$ is an unknown signal (disturbance, model uncertainty, etc.). The system can, also, be written in the following extended form (as in (11)):

$$\begin{aligned}\dot{\xi}(t) &= \begin{bmatrix} f\left(\zeta(t), v(\zeta(t) + \varepsilon_\zeta(t)), d(t)\right) \\ -f\left(\zeta(t), v(\zeta(t) + \varepsilon_\zeta(t)), d(t)\right) \end{bmatrix} = f_e(\xi(t), d(t)), \\ \xi(t_{i+1}^+) &= [\zeta^\top(t_{i+1}^+) \quad 0^\top]^\top,\end{aligned}\tag{36}$$

where $\xi = (\zeta, \varepsilon_\zeta) \in \mathbb{R}^{2n}$. Since $d(\cdot)$ admits infinite realizations, we may call (35) or (36) *family of ETC systems*. Additionally to Assumption 1, we assume that:

Assumption 3. For all $t \geq 0$: $d(t) \in \Delta$, where Δ is convex, compact and non-empty.

This assumption serves to impose existence and extendability of solutions of the DIs that we construct later on. For more information on this subject, the reader is referred to [29].

According to [13] and under Assumption 3, the family of systems (36) can be abstracted by a DI as follows:

$$\dot{\xi}(t) \in F_e(\xi(t)) := \{f_e(\xi(t), d(t)) : d(t) \in \Delta\}.\tag{37}$$

Here, given a point $x \in \mathbb{R}^n$, the inter-sampling time $\tau(x)$ is not uniquely defined, since it varies depending on the unknown signal $d(t)$. However, since we only care about lower and upper bounds on inter-sampling times, by employing DI (37) we can define the smallest and largest possible inter-sampling times of (36) (or DI (37)) as follows:

$$\tau^\downarrow(x) := \inf\left\{t > 0 : \exists \xi(t; x) \in \mathcal{Z}_{F_e}([0, t]; (x, 0)) \text{ such that } \phi(\xi(t; x)) \geq 0\right\},\tag{38}$$

$$\tau^\uparrow(x) := \inf\left\{t > 0 : \forall \xi(t; x) \in \mathcal{Z}_{F_e}([0, t]; (x, 0)), \exists \tau \in [0, t] \text{ such that } \phi(\xi(\tau; x)) \geq 0\right\}.\tag{39}$$

Observe the difference between $\tau^\downarrow(x)$ and $\tau^\uparrow(x)$: $\tau^\downarrow(x)$ is defined as the smallest time instant *when at least one trajectory* $\phi(\xi(t; x))$ hits zero, while $\tau^\uparrow(x)$ is defined as the smallest time instant *until when all possible trajectories* $\phi(\xi(t; x))$ have hit zero (recall that DIs generally have multiple solutions for a given initial condition).

Given the above definitions, we redefine the infinite-state system \mathcal{S} (13) such that it captures the traffic behaviour of the family of systems (35), as follows:

$$\mathcal{S} = (X, X_0, U, \longrightarrow, Y, H),\tag{40}$$

where $X, X_0 \subseteq \mathbb{R}^n$, U is a singleton, $Y \subseteq \mathbb{R}^+$, $H(x) = [\tau^\downarrow(x), \tau^\uparrow(x)]$ and $\longrightarrow \subseteq X \times X$ is defined such that $(x, x') \in \longrightarrow \iff x' \in \pi_\zeta \mathcal{X}_{H(x)}^{F_e}((x, 0))$, where π_ζ denotes projection to the ζ -variables. The problem statement now is constructing a finite-state abstraction of system (40):

Problem Statement 2. Consider the infinite-state system \mathcal{S} (40). Let Assumptions 1 and 3 hold. Construct a power quotient system $\mathcal{S}_{/Q} = (X_{/Q}, X_{0/Q}, U_{/Q}, \xrightarrow{/Q}, Y_{/Q}, H_{/Q})$, with $X_{/Q}, X_{0/Q}, U_{/Q}, Y_{/Q}$ as in Problem Statement 1 and:

- $(x_{/Q}, x'_{/Q}) \in \xrightarrow{/Q}$ if $\exists x \in x_{/Q}$ and $\exists x' \in x'_{/Q}$ such that $x' \in \pi_\zeta \mathcal{X}_{H(x)}^{F_e}(x)$,
- $H_{/Q}(\mathcal{R}_i) := [\underline{\tau}_i, \bar{\tau}_i]$, with:

$$\underline{\tau}_i \leq \inf_{x \in \mathcal{R}_i} \tau^\downarrow(x), \quad \bar{\tau}_i \geq \sup_{x \in \mathcal{R}_i} \tau^\uparrow(x). \quad (41)$$

The state-space partition is the same as in the previous case. Moreover, from Lemma 2.1, we again trivially obtain that $\mathcal{S} \stackrel{\epsilon}{\leq} \mathcal{S}_{/Q}$. In the following, we show that a slight adjustment to the technique proposed in Section 5 is enough to determine lower and upper bounds on inter-sampling times, and the state transitions, and thus address Problem Statement 2.

6.2 Lower Bounds on Inter-Sampling Times

First, DI (37) is rendered homogeneous of degree $\alpha > 0$ as follows:

$$\begin{aligned} \begin{bmatrix} \dot{\xi}(t) \\ \dot{w}(t) \end{bmatrix} &\in \tilde{F}_e(\xi(t), w(t)), \\ \tilde{F}_e(\xi, w) &:= \begin{bmatrix} \{w^{\alpha+1} f_e(w^{-1}\xi, d(t)) : d(t) \in \Delta\} \\ \{0\} \end{bmatrix}. \end{aligned} \quad (42)$$

Again, denoting the minimum and maximum inter-sampling times of DI (42) by $\tilde{\tau}^\downarrow(y), \tilde{\tau}^\uparrow(y)$ for $y \in \mathbb{R}^{n+1}$, we get that for $x \in \mathbb{R}^n$: $\tilde{\tau}^\downarrow((x, 1)) = \tau^\downarrow(x)$ and $\tilde{\tau}^\uparrow((x, 1)) = \tau^\uparrow(x)$, where $\tau^\downarrow(\cdot), \tau^\uparrow(\cdot)$ are the ones of DI (37). Given the minimum inter-sampling times $\tilde{\tau}^\downarrow(\cdot)$, in [13] isochronous manifolds of homogenized DIs (42) have been defined as in the previous: $M_{\tau_\star} := \{(x, w) \in \mathbb{R}^{n+1} : \tilde{\tau}^\downarrow((x, w)) = \tau_\star\}$. Furthermore, it has been proven that $\tilde{\tau}^\downarrow(\cdot)$ obeys the scaling law:

$$\tilde{\tau}^\downarrow(\lambda(x, w)) = \lambda^{-\alpha} \tilde{\tau}^\downarrow((x, w)).$$

Finally, as shown in [13], to derive inner-approximations of isochronous manifolds of DI (42), we could again use Theorem 4.1 by fixing $p = 1$ and slightly altering inequality (19a) such that it considers unknown signals that lie in Δ as follows:

$$\frac{\partial \tilde{\phi}}{\partial z}((z, w)) w^{\alpha+1} f_e(w^{-1}z, u) \leq \delta_0 \phi((z, w)) + \delta_1, \quad \forall (z, w, u) \in \Xi \times \Delta. \quad (43)$$

The main difference between (19a) and (43) is that in (43) only the first Lie derivative of $\tilde{\phi}$ is considered, since higher-order derivatives would require differentiability of the unknown signal $d(t)$, which is not a standard assumption to make.

Now that the homogenization procedure, the scaling law and the approximations of isochronous manifolds have been extended to perturbed uncertain ETC systems, the same procedure as in Section 5.1 and Proposition 5.1 can be followed (approximations of conic sections $\underline{M}_{\tau_\star} \cap \mathcal{C}_i$ by spherical segments \mathcal{S}_i , etc.), to determine lower bounds $\underline{\tau}_i$ such that:

$$\forall x \in \mathcal{R}_i : \quad \underline{\tau}_i \leq \tau^\downarrow(x).$$

Remark 8. *In the case of perturbed uncertain systems, only the first derivative of $\tilde{\phi}$ can be used. This can probably cause performance degradation (conservative lower bounds $\underline{\tau}_i$), compared to the previous, where p derivatives of $\tilde{\phi}$ are used. This is showcased in Section 7, via a numerical example. However, in cases where $d(t)$ is known to be differentiable and the derivatives of d are bounded (e.g. sinusoidal disturbances, uncertainties with bounded variations, etc.), higher-order derivatives could be considered.*

6.3 Upper Bounds on Inter-Sampling Times and Transitions

The reachability analysis tool Flow* [25] is able to handle systems with bounded disturbances and uncertainties. Furthermore, Proposition 5.3 trivially extends to perturbed uncertain systems. In other words, if $\mathcal{X}_{\tau_{i\max}}^{f_e}(\mathcal{I}_i) \cap \mathcal{U} = \emptyset$ for all $d(t) \in \Delta$, where $f_e(\cdot)$ is defined in (36) and the sets $\mathcal{I}_i, \mathcal{U}$ are defined in Proposition 5.3, then:

$$\forall x \in \mathcal{R}_i : \tau^\uparrow(x) \leq \tau_{i\max}.$$

Hence, by employing Flow*, we determine upper bounds $\bar{\tau}_i$ of inter-sampling times of (35) and the state transitions of \mathcal{S}/Q , using reachability analysis, as it was described in Section 5.2.

Remark 9. *Due to the presence of the unknown signal $d(t)$, the upper bound $\tau^\uparrow(x)$ of inter-sampling times for some regions \mathcal{R}_i might be $+\infty$ (e.g. when $d(t)$ cancels the nominal system's dynamics). Thus, the use of a heartbeat τ_h , as introduced in Remark 6, is mandatory. In this way, the upper bound for each region \mathcal{R}_i is determined by $\bar{\tau}_i = \min(\tau_{i\max}, \tau_h)$.*

7 Numerical Examples

In this section, we provide two numerical examples, demonstrating how our proposed methodology is applied. In particular, first we construct a traffic abstraction of a nonlinear non-homogeneous ETC system, without disturbances and uncertainties, using the procedure described in Section 5. Afterwards, we abstract the traffic of the same system, considering bounded disturbances as well, according to the technique developed in Section 6.

7.1 System without Disturbances or Uncertainties

Consider the following nonlinear ETC system:

$$\dot{\zeta}_1 = -\zeta_1, \quad \dot{\zeta}_2 = \zeta_1^2 + \zeta_2^3 + u,$$

with $u = -(\zeta_2 + \varepsilon_{\zeta_2}) - (\zeta_1 + \varepsilon_{\zeta_1})^2 - (\zeta_2 + \varepsilon_{\zeta_2})^3$ and a Lebesgue-sampling triggering function $\phi(\zeta(t), \varepsilon_\zeta(t)) = \varepsilon_\zeta^2 - 0.01^2$. Both of them satisfy Assumptions 1 and 2. First, the system and triggering function are homogenized according to the homogenization procedure (15)-(16):

$$\begin{bmatrix} \dot{\xi}(t) \\ \dot{w}(t) \end{bmatrix} = \begin{bmatrix} -\zeta_1(t)w^2(t) \\ \zeta_1^2(t)w(t) + \zeta_2^3(t) + \tilde{u} \\ \zeta_1(t)w^2(t) \\ -\zeta_1^2(t)w(t) - \zeta_2^3(t) - \tilde{u} \\ 0 \end{bmatrix}, \quad (44)$$

$$\begin{aligned} \tilde{u} &= -(\zeta_2 + \varepsilon_{\zeta_2})w^2(t) - (\zeta_1 + \varepsilon_{\zeta_1})^2w(t) - (\zeta_2 + \varepsilon_{\zeta_2})^3, \\ \tilde{\phi}(\xi(t), w(t)) &= \varepsilon_\zeta^2 - 0.01^2w^2(t). \end{aligned} \quad (45)$$

The degree of homogeneity for the homogenized system (44) and triggering function (45) is 2 and 1, respectively.

In order to create the traffic abstraction of the ETC system, we assume that the state space is the box $X = [-1, 1]^2$. We partition the state space into 49 equal boxes \mathcal{R}_i . According to the proposed methodology, to compute the inter-sampling times' lower bounds $\underline{\tau}_i$, first we compute an approximation \underline{M}_{τ^*} of an isochronous manifold of (44)-(45). We make use of Theorem 4.1 and select $Z = [-0.1, 0.1]^2$, $W = [10^{-7}, 0.1]$, $\rho = 0.099$ (such that $D_\rho \subset Z \times W$) and $p = 5$ (we use derivatives of $\tilde{\phi}$ of up to 5th order). Observe that $X \subset B = \{x \in \mathbb{R}^2 : |x| \leq 99 \cdot 10^4\}$, as required by Remark 3. To find the δ_i coefficients of Theorem 4.1 we employ the computational algorithm proposed in [12]. The obtained coefficients are: $\delta_0 = \delta_3 = \delta_4 = 0$, $\delta_1 \approx 9.9 \cdot 10^{-7}$, $\delta_2 \approx 9.8 \cdot 10^{-5}$ and $\delta_5 \approx 2 \cdot 10^{-5}$. Using the approximation $\underline{M}_{0.001}$, the timing lower bounds $\underline{\tau}_i$ are determined as described in Section 5.1 and Proposition 5.1. To derive the spherical segments S_i with the line-search algorithm described in Section 5.1, we employed the SMT solver dReal [33]. Indicatively, the timing lower bounds for some regions are: $\underline{\tau}_1 \approx 0.0035$, $\underline{\tau}_{11} \approx 0.0077$, $\underline{\tau}_{25} \approx 0.013$.

Afterwards, for the computation of timing upper bounds $\bar{\tau}_i$, the combination of a line search with reachability analysis is employed, as described in Section 5.2. For reachability analysis, we have used dReach [24]. We have also dictated an ad-hoc heartbeat $\tau_h = 0.025$, as instructed by Remark 6. The timing upper bounds of the same aforementioned regions $\mathcal{R}_1, \mathcal{R}_{11}, \mathcal{R}_{25}$ have been obtained as follows: $\bar{\tau}_1 \approx 0.01$, $\bar{\tau}_{11} \approx 0.023$, $\bar{\tau}_{25} \approx 0.025 = \tau_h$. Figure 4 depicts the timing lower and upper bounds for each region \mathcal{R}_i . The transitions of the abstraction are determined based on

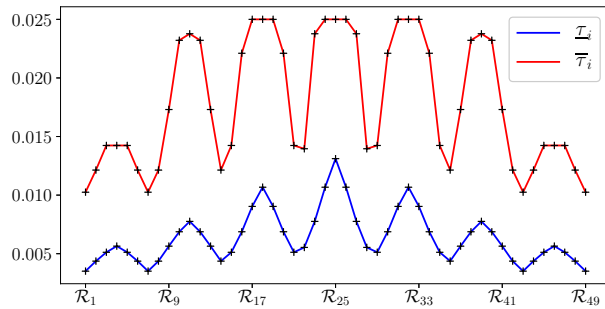


Figure 4: Lower bounds $\underline{\tau}_i$ and upper bounds $\bar{\tau}_i$ of inter-sampling times for each region \mathcal{R}_i .

the already computed reachable flowpipes of each region \mathcal{R}_i , as aforementioned. Figure 5 shows the transitions of the abstraction; each dotted point $(\mathcal{R}_i, \mathcal{R}_j)$ represents an existing transition from \mathcal{R}_i to \mathcal{R}_j . There are 327 transitions in total.

The constructed abstraction ϵ -approximately simulates the ETC system, for all $\epsilon \geq 0.01634 = \bar{\tau}_9 - \underline{\tau}_9$. To make our abstraction more precise, at the expense of heavier offline computations, we could: use a larger number of regions \mathcal{R}_i , choose a higher order of approximation p (which generally leads to more accurate lower bounds $\underline{\tau}_i$), decrease the step size of all the line searches employed, etc.

Finally, we have run a simulation to showcase the validity of our results. Specifically, the system is initialized at $(0.8, -0.8)$ and the simulation duration is 2s. Figure 6 depicts the simulation results. The red line is the evolution of the actual ETC inter-sampling times during the simulation, while the blue lines represent the intervals $[\underline{\tau}_i, \bar{\tau}_i]$ generated by the abstraction (by looking at which region \mathcal{R}_i did the state belong at the corresponding time instant, and plotting the corresponding interval).

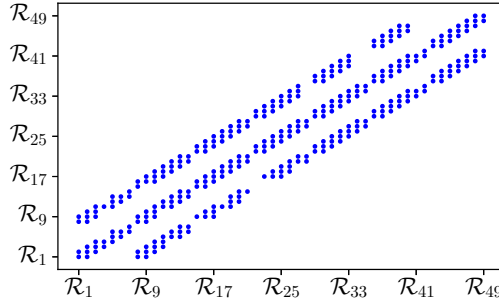


Figure 5: Transitions of the abstraction. Each dotted point $(\mathcal{R}_i, \mathcal{R}_j)$ represents a transition from \mathcal{R}_i to \mathcal{R}_j .

It is clear that the inter-sampling time is always confined in $[\underline{\tau}_i, \bar{\tau}_i]$, as expected. The inter-sampling times cap at $\tau_h = 0.025$. Furthermore, the system's trajectory followed the following spatial path: $\mathcal{R}_{43} \rightarrow \mathcal{R}_{43} \rightarrow \dots \rightarrow \mathcal{R}_{44} \rightarrow \mathcal{R}_{37} \rightarrow \mathcal{R}_{37} \rightarrow \dots \rightarrow \mathcal{R}_{38} \rightarrow \mathcal{R}_{31} \rightarrow \mathcal{R}_{31} \rightarrow \dots \rightarrow \mathcal{R}_{32} \rightarrow \mathcal{R}_{25} \rightarrow \mathcal{R}_{25} \rightarrow \dots$. The trajectory remained in the regions $\mathcal{R}_{43}, \mathcal{R}_{37}, \mathcal{R}_{31}, \mathcal{R}_{25}$ for a relatively large period, while the regions $\mathcal{R}_{44}, \mathcal{R}_{38}, \mathcal{R}_{32}$ were visited for a very short period of time (only one inter-sampling interval). That is why looking at Figure 6 it seems that the system visited 4 distinct regions. In fact, if we look closely, the transitions to regions $\mathcal{R}_{44}, \mathcal{R}_{38}, \mathcal{R}_{32}$ do show up in Figure 6, at times $t \approx 0.2s$, $t \approx 0.9s$, $t \approx 1.8s$ correspondingly, but they correspond to a very short period of time. Finally, observe that all transitions taken during the simulation are contained in the computed transition set of the abstraction, depicted in Figure 5.

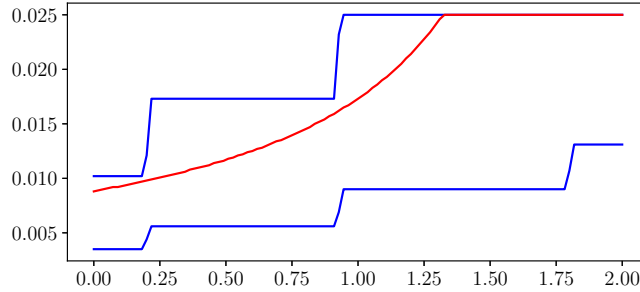


Figure 6: Time evolution of the ETC system's inter-sampling times (red line) and the bounding intervals $[\underline{\tau}_i, \bar{\tau}_i]$ (blue lines) generated by the abstraction, during a simulation.

7.2 System with Disturbances/Uncertainties

Now, consider a perturbed version of the previous system:

$$\dot{\zeta}_1 = -\zeta_1, \quad \dot{\zeta}_2 = \zeta_1^2 + \zeta_2^3 + u + d,$$

where u is as before and $d(t) \in [-0.1, 0.1] = \Delta$. We also consider the same triggering function. We construct the homogeneous DI abstracting the above family of perturbed ETC systems, as instructed

by (42):

$$\begin{aligned} \begin{bmatrix} \dot{\xi}(t) \\ \dot{w}(t) \end{bmatrix} &\in \tilde{F}_e(\xi(t), w(t)), \\ \tilde{F}_e(\xi, w) &:= \begin{bmatrix} \{w^3 f_e(w^{-1}\xi, d(t)) : d(t) \in \Delta\} \\ \{0\} \end{bmatrix}. \end{aligned}$$

Again, we partition the state space $X = [-1, 1]^2$ into 49 equal boxes \mathcal{R}_i . We determine the lower bounds $\underline{\tau}_i$ as described in Section 6.2. We select Z, W as before and we obtain the δ_0, δ_1 coefficients, that now satisfy (43) instead of (19a), as follows: $\delta_0 \approx 0.0509$ and $\delta_1 \approx 3.14 \times 10^{-6}$. Indicatively, timing lower bounds for some regions are: $\underline{\tau}_1 \approx 0.00035$, $\underline{\tau}_{11} \approx 0.00140$, $\underline{\tau}_{25} \approx 0.00300$. For the computation of the upper bounds, we employ reachability analysis with Flow* [25]. Moreover, we have dictated an ad-hoc heartbeat $\tau_h = 0.04$. Figure 7 depicts the results. Compared to the unperturbed case, we see that we have obtained considerably smaller timing lower bounds (some times an order of magnitude smaller). This is due to two reasons: First, the disturbance itself can cause smaller inter-sampling times (e.g. when it makes the vector field “faster”). Second, as commented in Remark 8, considering first order derivatives of $\tilde{\phi}$ may cause additional conservativeness, when computing timing lower bounds. Furthermore, we see that the computed upper-bounds are larger than in the previous case, as expected, due to the presence of the unknown disturbance.

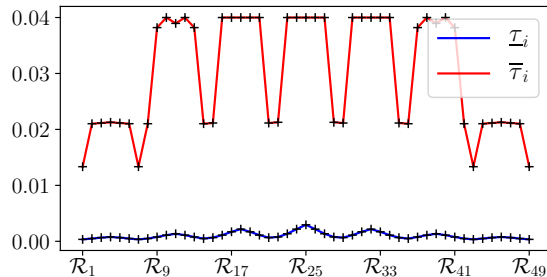


Figure 7: Lower bounds $\underline{\tau}_i$ and upper bounds $\bar{\tau}_i$ of inter-sampling times for each region \mathcal{R}_i .

Figure 8 depicts the transitions of the abstraction. Here, the total number of transitions is 361, approximately 10% larger than in the unperturbed case. Overall, we have $\mathcal{S} \stackrel{\epsilon}{\subseteq} \mathcal{S}_{/Q}$ for $\epsilon \geq 0.03889 = \bar{\tau}_9 - \underline{\tau}_9$, which is higher due to the unknown disturbance and the conservativeness that comes with it.

Finally, we run the same simulation as before, with the additive disturbance $d(t) = 0.1 \sin(10t)$. The results are depicted in Figure 9, which clearly shows that the actual ETC inter-sampling times are confined in the computed intervals $[\underline{\tau}_i, \bar{\tau}_i]$. We observe that, due to the disturbance, the actual inter-sampling times can vary greatly, even in the same region \mathcal{R}_i (e.g. observe the period from 1.2s to 1.6s in Figure 9). Thus, we have to emphasize that *the computed intervals $[\underline{\tau}_i, \bar{\tau}_i]$ are larger than in the unperturbed case, not only because of conservativeness in computing the lower bounds, but also because of the very presence of the unknown signal $d(t)$* . In other words, up to a certain extent, the conservativeness of the intervals $[\underline{\tau}_i, \bar{\tau}_i]$ in the case of perturbed uncertain systems is structural. Finally, the trajectory followed the spatial path: $\mathcal{R}_{43} \rightarrow \mathcal{R}_{43} \rightarrow \dots \rightarrow \mathcal{R}_{44} \rightarrow \mathcal{R}_{37} \rightarrow \mathcal{R}_{37} \rightarrow \dots \rightarrow \mathcal{R}_{31} \rightarrow \mathcal{R}_{31} \rightarrow \dots \rightarrow \mathcal{R}_{32} \rightarrow \mathcal{R}_{32} \rightarrow \mathcal{R}_{25} \rightarrow \mathcal{R}_{25} \rightarrow \dots$. These transitions are indeed contained in the abstraction’s transition set, as shown in Figure 8.

It is worth noting that the complete construction of the above abstractions (both the perturbed

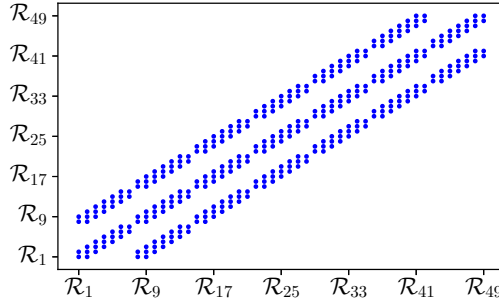


Figure 8: Transitions of the abstraction. Each dotted point $(\mathcal{R}_i, \mathcal{R}_j)$ represents a transition from \mathcal{R}_i to \mathcal{R}_j .

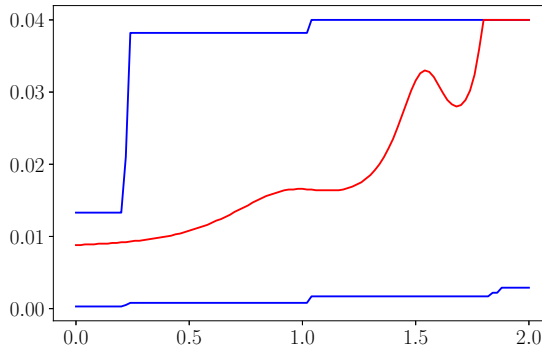


Figure 9: Time evolution of the perturbed ETC system's inter-sampling times (red line) and the bounding intervals $[\underline{\tau}_i, \bar{\tau}_i]$ generated by the abstraction, during a simulation.

and the unperturbed case) amounted to approximately 30-50 minutes of computation time (for each abstraction) on a Macbook Pro 2017. The code implementing the above is written in Python.

8 Discussion and Future Work

Prior to this work, versatile scheduling of communication traffic in networks of ETC loops, as proposed in [23], was only applicable to LTI systems [22] with quadratic triggering functions. Here, we significantly extended this framework, by constructing traffic abstractions of general nonlinear ETC systems with disturbances, uncertainties and general triggering functions. As expected, we observe in the performed simulations, that the abstractions are more conservative in the case of perturbed uncertain systems, as they need to provide hard worst-case guarantees. Thus, future work will be devoted to improve abstractions of perturbed uncertain systems.

Furthermore, according to numerous simulations that we have performed, the abstractions are computed in relatively short time (approximately 10-60 minutes) for systems of small dimensionality (2-d or 3-d), with a conventional personal computer. To further improve the computation time, future research will also focus on constructing abstractions that scale better with the dimension of the system (this has been carried out for LTI periodic event-triggered control systems in [35]). To

construct scalable abstractions, we could employ something that is also used in [26]: the sets which are delimited by two approximations of isochronous manifolds $\underline{M}_{\tau_i}, \underline{M}_{\tau_{i+1}}$ (with $\tau_i < \tau_{i+1}$) admit τ_i as a uniform lower bound on inter-sampling times (see [12, 13]). Thus, instead of partitioning the state-space into polytopes, we could a-priori dictate a finite set of lower-bounds $\{\tau_1, \dots, \tau_q\}$ and define the regions \mathcal{R}_i as the sets that are delimited by consecutive approximations \underline{M}_{τ_i} of isochronous manifolds M_{τ_i} . In this way, the state-space partitioning does not scale exponentially with the dimensionality of the system, and the whole step of computing lower bounds on inter-sampling times for each region \mathcal{R}_i is skipped. This poses a new challenge: the regions \mathcal{R}_i are now big sets that look like spherical shells centered at the origin (if we assume that the origin is the equilibrium), which might degrade the performance of reachability analysis tools. To cope with that, in [26] the regions \mathcal{R}_i were further partitioned via a conic covering, which again scales exponentially with the dimensions of the system.

9 Appendix

9.1 Technical Proofs

Proof of Proposition 4.1. System (15) is homogeneous, which implies that the scaling law (12) applies. From Theorem 4.1, for all points $y := (x, w) \in \underline{M}_{\tau_\star} \cap \mathcal{C}$: $\exists! \kappa_y \geq 1$ s.t. $\kappa_y y \in M_{\tau_\star}$. But, since $\kappa_y y \in M_{\tau_\star}$, we have that $\tilde{\tau}(\kappa_y y) = \tau_\star$ (by definition of isochronous manifolds M_{τ_\star}). Thus, by the scaling law (12), we get that for all $y \in \underline{M}_{\tau_\star} \cap \mathcal{C}$:

$$\tilde{\tau}(y) = \tilde{\tau}(\kappa_y^{-1} \kappa_y y) = \kappa_y^\alpha \tilde{\tau}(\kappa_y y) = \kappa_y^\alpha \tau_\star \geq \tau_\star. \quad (46)$$

For a point $(x_0, 1) \in \mathcal{C}$, there exists $\lambda > 0$ such that $\lambda(x_0, 1) \in \underline{M}_{\tau_\star} \cap \mathcal{C}$ (see Figure 1). Thus, by the scaling law and (46), we obtain $\tilde{\tau}((x_0, 1)) \geq \lambda^\alpha \tau_\star$. Finally, from (17) $\tau(x_0) = \tilde{\tau}((x_0, 1)) \geq \lambda^\alpha \tau_\star$. \square

Proof of Proposition 5.1. By the scaling law (12), following the same steps as in (23), since S_i inner-approximates $\underline{M}_{\tau_\star} \cap \mathcal{C}_i$, we have that:

$$\forall y \in S_i : \tau(y) \geq \tau_\star. \quad (47)$$

Now, observe that for all $(x, 1) \in \tilde{\mathcal{R}}_i$ there exists unique $\lambda_{(x,1)} \geq 1$ such that $\lambda_{(x,1)}(x, 1) \in S_i$ (owing to (26) and (27)). In fact, since S_i is a spherical segment, then $\lambda_{(x,1)} = \frac{r_i}{|(x,1)|}$. Then, by the scaling law (12) again, for all $(x, 1) \in \tilde{\mathcal{R}}_i$:

$$\tilde{\tau}((x, 1)) = \lambda_{(x,1)}^\alpha \tilde{\tau}(\lambda_{(x,1)}(x, 1)) \geq \left(\frac{r_i}{|(x,1)|} \right)^\alpha \tau_\star.$$

Moreover, by (28), we can conclude that for all $(x, 1) \in \tilde{\mathcal{R}}_i$:

$$\tilde{\tau}((x, 1)) \geq \left(\frac{r_i}{|(x_{i_\star}, 1)|} \right)^\alpha \tau_\star.$$

Finally, from (17), we have:

$$\forall x \in \mathcal{R}_i : \tau(x) \geq \left(\frac{r_i}{|(x_{i_\star}, 1)|} \right)^\alpha \tau_\star.$$

\square

Proof of Proposition 5.2. Observe that $\mu((x, w), t)$, by construction, satisfies the scaling property:

$$\mu(\lambda(x, w), t) = \lambda^{\theta+1} \mu((x, w), \lambda^\alpha t). \quad (48)$$

Moreover, as it has been proven in [12], $\mu((x, w), t)$ is an increasing function w.r.t. t .

Consider any point $(x_0, w_0) \in \mathcal{C}_i$ with $\mu((x_0, w_0), \tau_\star) \leq 0$. We will prove that there exists a unique $\lambda \geq 1$ such that $\lambda \cdot (x_0, w_0) \in \underline{M}_{\tau_\star} \cap \mathcal{C}_i$: As it has been proven in [12], there exists unique $\tau_{(x_0, w_0)}$ such that $\mu((x_0, w_0), \tau_{(x_0, w_0)}) = 0$. Since μ is increasing w.r.t. t and $\mu((x_0, w_0), \tau_\star) \leq 0$, then $\tau_{(x_0, w_0)} \geq \tau_\star$. Let $\lambda = \left(\frac{\tau_{(x_0, w_0)}}{\tau_\star}\right)^{\frac{1}{\alpha}} \geq 1$ (since $\alpha > 0$). Then, from (48), for the point $\lambda \cdot (x_0, w_0)$ we have:

$$\begin{aligned} \mu(\lambda \cdot (x_0, w_0), \tau_\star) &= \lambda^{\theta+1} \mu((x_0, w_0), \lambda^\alpha \tau_\star) \\ &= \lambda^{\theta+1} \mu((x_0, w_0), \tau_{(x_0, w_0)}) = 0, \end{aligned}$$

i.e. $\lambda \cdot (x_0, w_0) \in \underline{M}_{\tau_\star}$. Moreover, $(x_0, w_0) \in \mathcal{C}_i \implies \lambda \cdot (x_0, w_0) \in \mathcal{C}_i$. Thus, $\lambda \cdot (x_0, w_0) \in \underline{M}_{\tau_\star} \cap \mathcal{C}_i$. Consequently, by (30), we can conclude that:

$$\forall (x, w) \in S_i : \quad \exists! \lambda \geq 1 \text{ such that } \lambda \cdot (x, w) \in \underline{M}_{\tau_\star} \cap \mathcal{C}_i,$$

i.e. S_i inner-approximates $\underline{M}_{\tau_\star} \cap \mathcal{C}_i$. □

References

- [1] K.-E. Åarżén, “A simple event-based pid controller,” *IFAC Proceedings Volumes*, vol. 32, no. 2, pp. 8687–8692, 1999.
- [2] W. Heemels, R. Gorter, A. Van Zijl, P. Van den Bosch, S. Weiland, W. Hendrix, and M. Vonder, “Asynchronous measurement and control: a case study on motor synchronization,” *Control Engineering Practice*, vol. 7, no. 12, pp. 1467–1482, 1999.
- [3] K. J. Astrom and B. M. Bernhardsson, “Comparison of riemann and lebesgue sampling for first order stochastic systems,” in *Proceedings of the 41st IEEE Conference on Decision and Control, 2002.*, vol. 2. IEEE, 2002, pp. 2011–2016.
- [4] P. Tabuada, “Event-triggered real-time scheduling of stabilizing control tasks,” *IEEE Transactions on Automatic Control*, vol. 52, no. 9, pp. 1680–1685, 2007.
- [5] J. Lunze and D. Lehmann, “A state-feedback approach to event-based control,” *Automatica*, vol. 46, no. 1, pp. 211–215, 2010.
- [6] T. Liu and Z.-P. Jiang, “A small-gain approach to robust event-triggered control of nonlinear systems,” *IEEE Transactions on Automatic Control*, vol. 60, no. 8, pp. 2072–2085, 2015.
- [7] A. Girard, “Dynamic triggering mechanisms for event-triggered control,” *IEEE Transactions on Automatic Control*, vol. 60, no. 7, pp. 1992–1997, 2015.

- [8] M. Velasco, J. Fuertes, and P. Marti, “The self triggered task model for real-time control systems,” in *Work-in-Progress Session of the 24th IEEE Real-Time Systems Symposium*, vol. 384, 2003.
- [9] X. Wang and M. D. Lemmon, “Self-triggered feedback control systems with finite-gain l_2 stability,” *IEEE Transactions on Automatic Control*, vol. 54, no. 3, pp. 452–467, 2009.
- [10] M. Mazo Jr., A. Anta, and P. Tabuada, “An iss self-triggered implementation of linear controllers,” *Automatica*, vol. 46, no. 8, pp. 1310–1314, 2010.
- [11] A. Anta and P. Tabuada, “To sample or not to sample: Self-triggered control for nonlinear systems,” *IEEE Transactions on Automatic Control*, vol. 55, no. 9, pp. 2030–2042, 2010.
- [12] G. Delimpaltadakis and M. Mazo, “Isochronous partitions for region-based self-triggered control,” *IEEE Transactions on Automatic Control*, pp. 1–1, 2020.
- [13] G. Delimpaltadakis and M. Mazo Jr, “Region-based self-triggered control for perturbed and uncertain nonlinear systems,” *arXiv preprint arXiv:2005.00473*, 2020.
- [14] W. P. M. H. Heemels, K. H. Johansson, and P. Tabuada, “An introduction to event-triggered and self-triggered control,” in *Proceedings of the IEEE Conference on Decision and Control*, 2012, pp. 3270–3285.
- [15] G. C. Buttazzo, G. Lipari, and L. Abeni, “Elastic task model for adaptive rate control,” in *Proceedings 19th IEEE Real-Time Systems Symposium (Cat. No. 98CB36279)*. IEEE, 1998, pp. 286–295.
- [16] M. Caccamo, G. Buttazzo, and L. Sha, “Elastic feedback control,” in *Proceedings 12th Euromicro Conference on Real-Time Systems. Euromicro RTS 2000*. IEEE, 2000, pp. 121–128.
- [17] R. Bhattacharya and G. J. Balas, “Anytime control algorithm: Model reduction approach,” *Journal of Guidance, Control, and Dynamics*, vol. 27, no. 5, pp. 767–776, 2004.
- [18] D. Fontanelli, L. Greco, and A. Bicchi, “Anytime control algorithms for embedded real-time systems,” *Lecture Notes in Computer Science (including subseries Lecture Notes in Artificial Intelligence and Lecture Notes in Bioinformatics)*, vol. 4981 LNCS, pp. 158–171, 2008.
- [19] S. Al-Areqi, D. Görges, and S. Liu, “Event-based networked control and scheduling codesign with guaranteed performance,” *Automatica*, vol. 57, pp. 128–134, 2015.
- [20] C. Lu, J. A. Stankovic, S. H. Son, and G. Tao, “Feedback control real-time scheduling: Framework, modeling, and algorithms,” *Real-Time Systems*, vol. 23, no. 1-2, pp. 85–126, 2002.
- [21] A. Cervin and J. Eker, “Control-scheduling codesign of real-time systems: The control server approach,” *Journal of Embedded Computing*, vol. 1, no. 2, pp. 209–224, 2005.
- [22] A. S. Kolarijani and M. Mazo, “Formal traffic characterization of lti event-triggered control systems,” *IEEE Transactions on Control of Network Systems*, vol. 5, no. 1, pp. 274–283, 2016.
- [23] A. S. Kolarijani, D. Adzkiya, and M. Mazo, “Symbolic abstractions for the scheduling of event-triggered control systems,” in *2015 54th IEEE Conference on Decision and Control (CDC)*. IEEE, 2015, pp. 6153–6158.

- [24] S. Kong, S. Gao, W. Chen, and E. Clarke, “dreach: δ -reachability analysis for hybrid systems,” in *International Conference on TOOLS and Algorithms for the Construction and Analysis of Systems*. Springer, 2015, pp. 200–205.
- [25] X. Chen, E. Ábrahám, and S. Sankaranarayanan, “Flow*: An analyzer for non-linear hybrid systems,” in *International Conference on Computer Aided Verification*. Springer, 2013, pp. 258–263.
- [26] G. Delimpaltadakis and M. Mazo Jr, “Traffic abstractions of nonlinear homogeneous event-triggered control systems,” *arXiv preprint arXiv:2003.09361*. To appear in *IEEE Conference on Decision and Control (CDC)*, 2020.
- [27] A. Anta and P. Tabuada, “Exploiting isochrony in self-triggered control,” *IEEE Transactions on Automatic Control*, vol. 57, no. 4, pp. 950–962, 2012.
- [28] G. Ewald, *Combinatorial convexity and algebraic geometry*. Springer Science & Business Media, 2012, vol. 168.
- [29] A. F. Filippov, *Differential Equations with Discontinuous Righthand Sides*. Kluwer Academic Publishers, Dordrecht, 1988.
- [30] P. Tabuada, *Verification and control of hybrid systems: a symbolic approach*. Springer Science & Business Media, 2009.
- [31] M. Kawski, “Geometric homogeneity and stabilization,” in *Nonlinear Control Systems Design 1995*. Elsevier, 1995, pp. 147–152.
- [32] E. Bernuau, D. Efimov, W. Perruquetti, and A. Polyakov, “On an extension of homogeneity notion for differential inclusions,” in *2013 European Control Conference (ECC)*. IEEE, 2013, pp. 2204–2209.
- [33] S. Gao, S. Kong, and E. M. Clarke, “dreal: An smt solver for nonlinear theories over the reals,” in *International Conference on Automated Deduction*. Springer, 2013, pp. 208–214.
- [34] K. Fukuda and A. Prodon, “Double description method revisited,” in *Franco-Japanese and Franco-Chinese Conference on Combinatorics and Computer Science*. Springer, 1995, pp. 91–111.
- [35] G. d. A. Gleizer and M. Mazo Jr, “Scalable traffic models for scheduling of linear periodic event-triggered controllers,” *arXiv preprint arXiv:2003.07642*, 2020.